Electronic Supplementary Material (ESI) for Environmental Science: Nano.

Influence of engineered nanomaterials on deposition and detachment of *Escherichia coli* in two model systems

Supporting Information

Table of Contents

Sand Preparation and Column Operation..........2
Syringe Pumps..........3
Instrument Limitation: Not Allowing Multiple Refractive Indices..........3
DLVO Modeling..........3
DLVO Modeling..........3
DLVO Shortcomings..........6
***E. coli* Deposition Mechanisms**..........7
DLVO Modeling Assumptions and Qualifications..........10
References Cited..........11

Sand Preparation and Column Operation

Sand was prepared as described previously, except that baked sand was not stored under vacuum between baking and rehydration[1]. Briefly, quartz (IOTA) was sieved and the fraction between 250 and 300 µm sieves was retained and soaked in 12 M HCl for at least 24 hours. Acid-soaked sand was washed with DI H2O and baked in an oven at 800 °C for at least 8 hours. The baked sand was rehydrated for at least one hour by boiling in DI water and it was stored in DI water until used when wet packing the column. The column had a length of 5 cm, inner diameter of 1.5 cm, and porosity of 0.45 +/- 0.01.

In preparation for column experiments, at least 40 mL (10 PV) of DI H2O were flowed through the column, followed by at least 40 mL (10 PV) of 10 mM KCl. Once UV-VIS measurements began, 30 mL of the experimental solution (7.5 PV), 30 mL of the KCl electrolyte (7.5 PV), and 20 mL of DI H2O (5 PV) were flowed through the column. Once each experiment was completed, the column was removed from the flow system and the experimental solution was flowed through the tubing to measure C_0 for the breakthrough curve using the same UV-VIS detector.

The detector scanned at 366 and 600 nm so that the composition of the effluent could be probed. Previous research has used these two wavelengths to study the photocatalytic activity of TiO_2 and measure the optical density of bacteria, respectively[2, 3]. During measurements of experimental C_0 values, suspensions containing *E. coli* O157:H7 alone or in the presence of either particle displayed a ratio of absorbance at 366 nm vs. 600nm that was greater than one. Meanwhile, both ENMs in the absence of bacteria displayed an absorbance ratio less than 1.

Syringe Pumps

Solutions were pumped through the column using syringe pumps (kd Scientific KDS 230) to reduce the pulsation of flow caused by peristaltic pumps, which have been used in past experiments[1]. Experimental solutions were not stirred or sonicated while held in syringes. An additional experiment was run to support the validity of using syringe pumps without stirring or sonication, showing that the C_0 for the *E. coli* O157:H7 and *E. coli* O157:H7 + TiO_2 scenarios changed less than 3% over a length of time similar to an experiment.

Instrument Limitation: Not Allowing Multiple Refractive Indices

The inability to account for multiple refractive indices within one measurement is a significant limitation of using dynamic light scattering (DLS) to assess particle size when using mixed-particle systems, such as those used in this work. In general, absolute values of cell-nanoparticle aggregate diameters measured by dynamic light scattering are most useful for the observation of trends, rather than drawing any major conclusion based on their absolute values.

For the mixture of *E. coli* O157:H7 and TiO_2, DLS measurements indicate the effective size of the bacteria is much smaller than that for bacteria in the presence of CuO. However, no significant changes in bacteria cell size are observed in SEM imaging of the *E. coli* O157:H7 and TiO_2 mixtures. Previous work by Chowdhury *et al.* (2012) employed similar conditions (including nano-TiO_2, *E. coli* O157:H7 cells, and 10 mM KCl background solution) and observed a similar trend. Specifically, the authors concluded that "electrostatic and electrosteric repulsion between nano-TiO_2 particles and bacteria can increase nano-TiO_2 aggregate size and decrease nano-TiO_2-bacteria aggregate size due to change in collisions of nano-TiO_2 aggregates." Therefore, it is hypothesized that the higher refractive index of TiO_2, compared to *E. coli* O157:H7 or CuO, may allow larger TiO_2 aggregates dominate dynamic light scattering measurements. This may contribute to the smaller recorded effective diameter of the nano-TiO_2-bacteria aggregates due to the large discrepancy in refractive index of TiO_2 (2.8), compared to bacteria (1.0) and CuO (0.86). It is hypothesized that the smaller effect of TiO_2 on DLS size measurements of *E. coli* 25922 is due to the TiO_2 being more covered by EPS in this scenario.

Bacteria:Nanoparticle Number Ratio Calculations

Table S1. Calculations of number ratio of bacteria to nanoparticles.

Particle Concentrations of TiO_2	
[TiO_2](mg/mL)	0.01
Density of anatase TiO_2 (mg/cm3)	3900
TiO_2 Particle radius (cm/particle)	0.0000061
TiO_2 Volume (cm3/particle)	9.50776E-16
Primary particles TiO_2/mL solution:	2.70E+09
Particle Concentrations of CuO	
[CuO](mg/mL)	0.01
Density of CuO (mg/cm3)	6315
CuO Particle radius (cm/particle)	0.0000025
CuO Volume (cm3/particle)	6.54498E-17
Primary particles CuO/mL solution:	2.42E+10
Bacteria:Nanoparticle Ratios	
TiO_2 primary particles per 10^9 cells / mL:	2.7
Cuo primary particles per 10^9 cells / mL:	24.2

DLVO Modeling

The interaction energy profiles for particle-particle, particle-spinach, and particle-quartz systems are presented in figures S1, S2, and S3, respectively. DLVO modeling predicted key aspects of experimental results. As indicated by SEM images and Figure S1, both nanoparticles appear to interact with both bacteria species in suspension. Also, the breakthrough curves for *E. coli* O157:H7 alone and in the presence of CuO are consistent with the primary minimum deposition predicted by DLVO theory. In addition, more column elution was observed during the DI H_2O rinse of the *E. coli* + TiO_2 scenario than during the other scenarios with the pathogen. UV-VIS adsorption analysis revealed that *E. coli* was the main species appearing in the effluent. Therefore, the pathogen was more stable in the presence of TiO_2, as predicted in Figure S3.

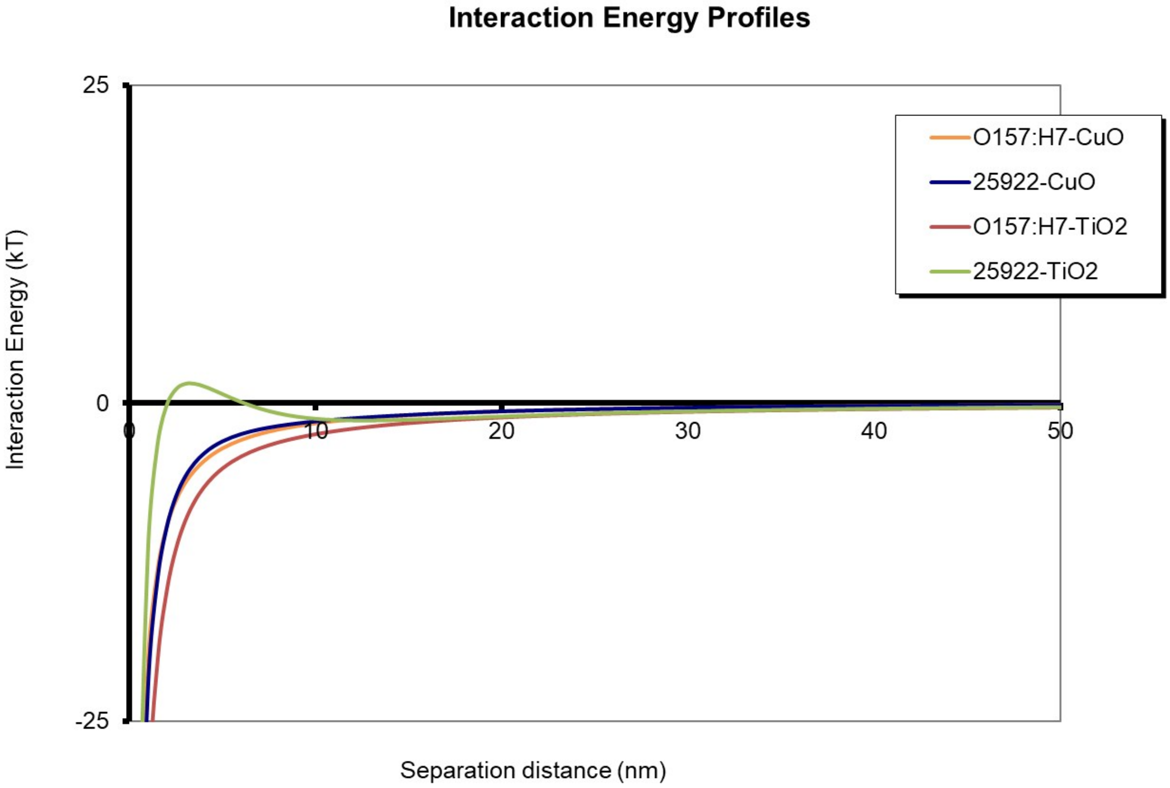

Figure S1. Particle-Particle DLVO for bacteria and ENMs.

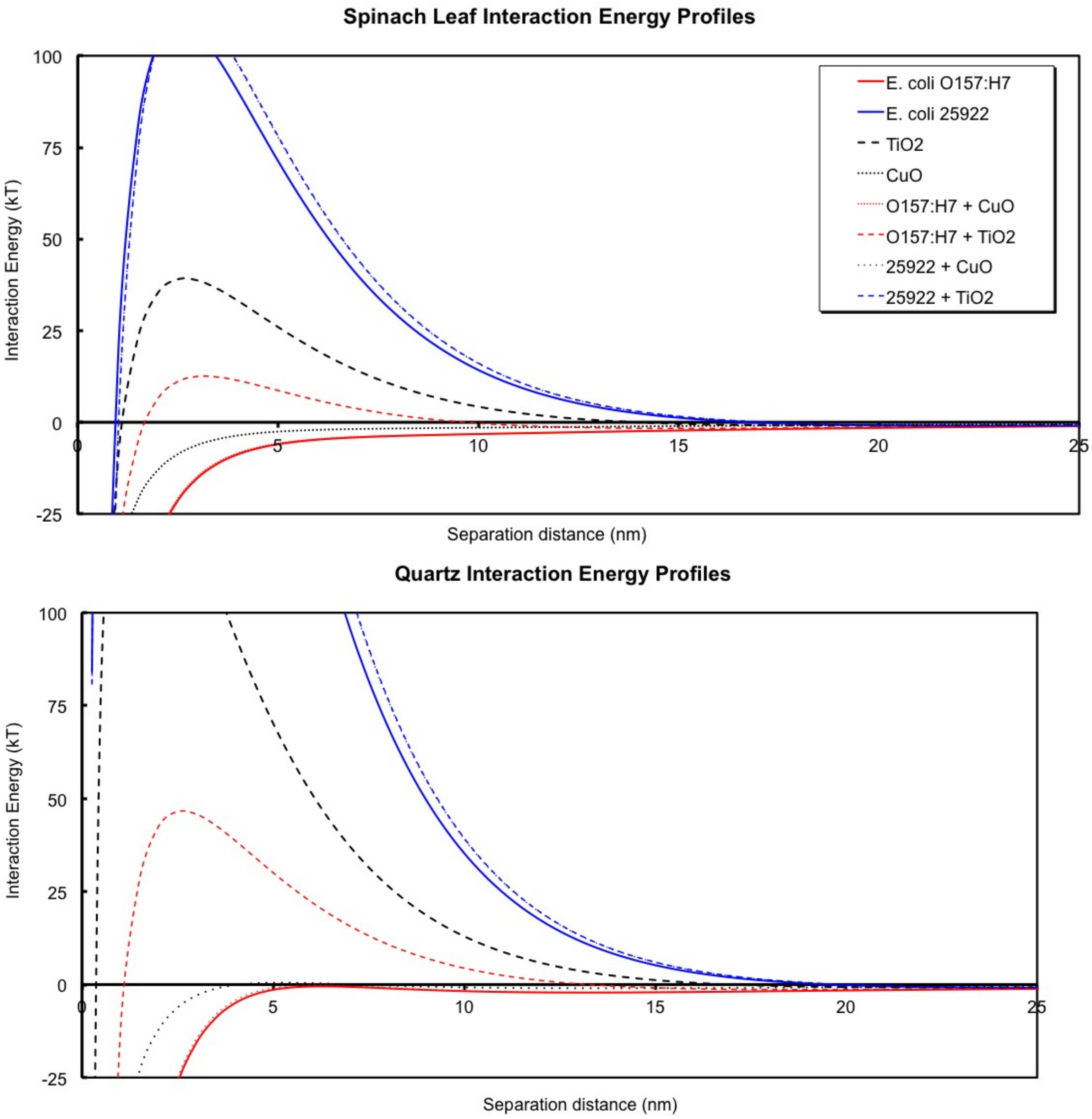

Figure S2. Particle-Plate DLVO for spinach leaf surface (top) and quartz sand surface (bottom).

An initial interpretation of DLVO results may lead the reader to conclude that most of the *E. coli* O157:H7 in the presence of TiO_2 should elute during the H_2O rinse. This would be a rational conclusion since a previous study with *E. coli* retained in a saturated sand column under unfavorable deposition conditions showed that the majority of bacteria were eluted from the column upon decreasing the ionic strength of the pore fluid, behavior consistent with secondary minimum deposition[1]. However, in the current study, only a fraction of the *E. coli* in the presence of TiO_2 elutes during the DI H_2O rinse.

It is likely that only a small portion of the *E. coli* O157:H7 cells have meaningful interaction with TiO_2. Based on the hydrodynamic diameter of TiO_2 in the absence of *E. coli*, TiO_2 concentration is estimated to be 10^7 aggregates/mL, while the *E. coli* O157:H7 is present at 10^9 cells/mL. Therefore, it is logical that the majority of the cells exhibit behavior that is consistent with DLVO predictions for *E. coli* in the absence of TiO_2.

DLVO Shortcomings

Based on DLVO predictions, *E. coli* O157:H7 should irreversibly deposit onto the spinach and quartz surfaces, due to its nearly neutral cell surface charge. Meanwhile, more highly charged *E. coli* 25922 should experience greater repulsive forces, so it should attach less and detach more. Instead, attachment rate coefficients onto spinach are around the same magnitude for both the pathogen and non-pathogen scenarios in the flow cell. Also, significant detachment of *E. coli* O157:H7 cells is observed in the flow cell (up to 18% of attached cells), while essentially no detachment of *E. coli* 25922 is observed. In addition, only partial release of *E. coli* 25922 is observed in the column (62% retention after DI rinse).

Similarly, the presence of TiO2 in suspension with *E. coli* O157:H7 is predicted to hinder irreversible bacteria attachment. However, TiO_2 has little effect on the pathogen's attachment and detachment in the flow cell. Moreover, *E. coli* O157:H7 exhibits a likely increase in retention in the column in the presence of TiO_2.These observations indicate DLVO interactions are not the primary factors influencing bacterial adhesion. This is in agreement with previous work[4].

A further shortcoming of DLVO modeling is that it predicts the elution of the majority of TiO_2 in the column in the absence of *E. coli*. However, little TiO_2 release was observed. Similar behavior of food grade TiO_2 was previously observed[5]. This behavior may be due to hydrophobic interactions of the TiO_2 nanoparticles.

E. coli Deposition Mechanisms

Some hypotheses for DLVO failing to predict *E. coli* deposition/detachment trends are based on physical shortcomings of the theory. Previous work found that colloid deposition kinetics were insensitive to particle size, despite DLVO theory predicting a decrease in particle deposition with increasing particle size[6]. It is possible that DLVO over-estimates the interaction energy for bacteria (relatively large particles) with surfaces. Furthermore, the equation that was used for van der Waals attraction between *E. coli* and surfaces in DLVO predictions, which assumes sphere-plate geometry, may under-estimate their attraction. Rod-shaped *E. coli* are expected to have greater van der Waals attraction to a surface than their spherical counterpart[7].

Other hypotheses for *E. coli* deposition deviating from DLVO theory are biological in nature. Cell surface heterogeneity and bacteria population heterogeneity may provide for primary minimum deposition in spite of DLVO calculations[1]. In addition, the larger amount of EPS observed with *E. coli* 25922 (Figure 1) may facilitate additional surface interactions with quartz, irrespective of charge barriers.

Size exclusion was not expected to play a significant role in transport within the column studies, based on previous work by Bradford *et al.* (2006)[9]. Bradford *et al.* specifically assessed the straining of *E. coli* O157:H7 in sand column experiments with varied quartz grain sizes and found that bacterial cells were physically strained when the quartz diameter was 240 microns, but was not significant strained when the sand diameter was 360 µm, unless the Darcy velocity value was small (<0.05 cm/min). For comparison, the experiments in this study utilized an average grain size of 275 µm and a relatively large Darcy velocity (1 cm/min), minimizing the likelihood that straining plays a major role for either the bacteria, nanoparticle, or their aggregates.

Further, Bradford *et al.* (2006) demonstrated a correlation between non-monotonic deposition profiles and suspected straining. Therefore, the smooth shape of our retention profile (which is non-monotonic) for *E. coli* O157:H7 with and without nanoparticles would suggest that size exclusion is not occurring. In contrast, extra EPS may contribute to the larger *E. coli* 25922 aggregates observed in DLS measurements, and thus physical straining may occur in this case. The straining hypothesis for *E. coli* 25922 in the column is supported by the bumpy retention profile shown in Figure S4. In the hypothetical absence of straining, there is already a hypothesized difference between *E. coli* O157:H7 and *E. coli* 25922 retention profiles: the *E. coli* 25922 retention profile may be less consistent with classical colloid filtration theory due to repulsive DLVO interactions[8].

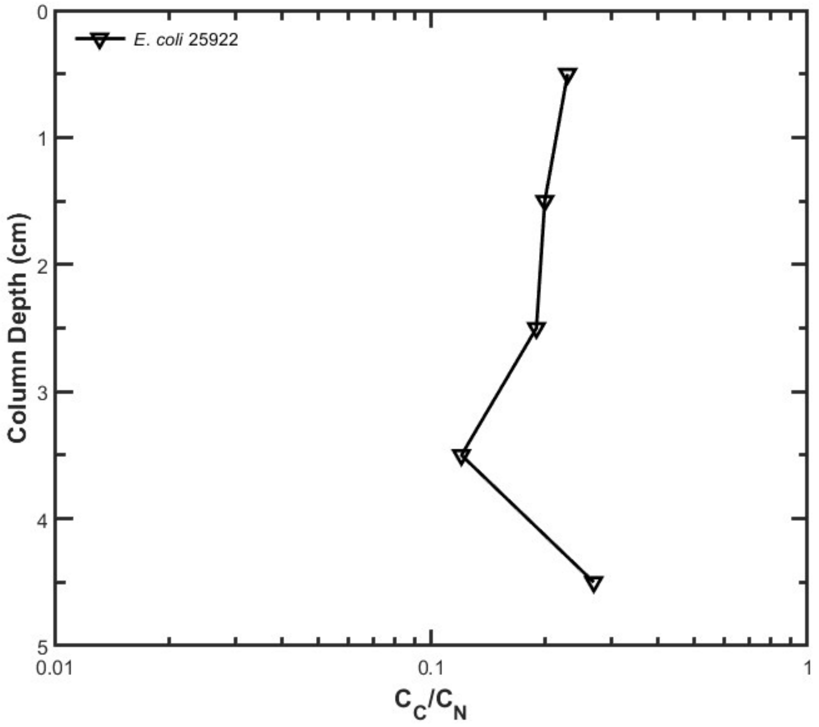

Figure S3. Column retention profile for column transport experiment with *E. coli* 25922. C_C and C_N are defined as concentration of recovered particles and the sum of concentrations of recovered particles for a given suspension, respectively. A depth of 0 cm corresponds to the entrance of the column.

However, the bumpy nature of the *E. coli* 25922 retention profile is different than the hypothesized deviation from classical colloid filtration theory. In previous work, a correlation can be seen between bumpy column deposition profiles and straining of *E. coli*[9]. In this work, bumpy column deposition profiles often coincided with breakthrough curves that had an upward-sloping breakthrough plateau, as seen in the *E. coli* 25922 scenario of Figure S5. Furthermore, it is logical that the slightly larger *E. coli* 25922 would be strained in 275 µm sand grains when previous work showed that *E. coli* O157:H7 was strained in 240 µm sand grains[9]. Other potential reasons for non-exponential deposition profiles are discussed elsewhere[9].

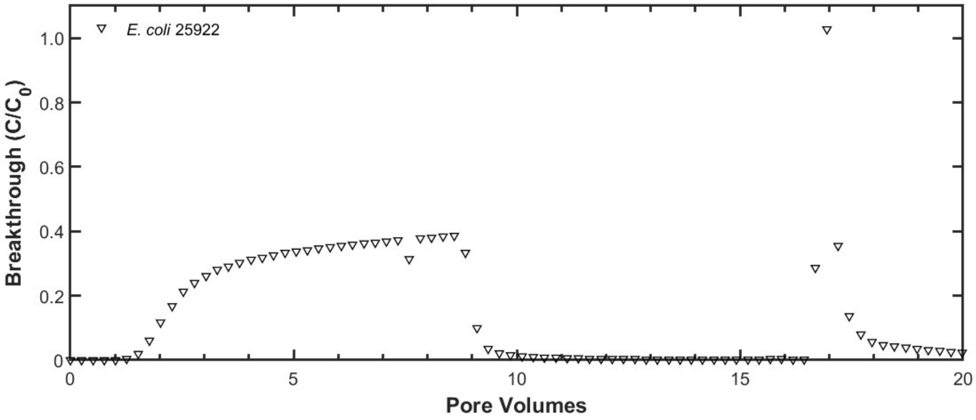

Figure S4. Breakthrough curve for saturated sand column transport experiment with *E. coli* 25922. Columns were injected with 10^9 cells/mL in 10 mM KCl electrolyte at pH 7. There are no error bars because only one replicate was completed. Experimental conditions: Darcy velocity = 1 cm/min, Pe = 65[10], bed length = 5 cm, bed diameter = 1.5 cm, porosity = 0.44, average grain diameter = 275µm.

DLVO Modeling Assumptions and Qualifications

Calculations of effective hydrodynamic diameter and zeta potential were used to generate DLVO predictions. Zeta potentials of -5 and -25 mV were used as estimates of net charges for spinach surfaces and quartz grains, respectively, based on previous work[1, 11].

The Van der Waals equation used in DLVO modeling of sphere-plate interaction is valid for separation distances of up to about 20% of the sphere radius[12]. For the limiting case of CuO nanoparticles, the DLVO calculations are estimated to be valid up to 47 nm (based on hydrodynamic diameter), by which point the DLVO curve is asymptotic.

The electrical double layer (EDL) equation used in the DLVO modeling of sphere-plate interaction is exact for surface potentials less than 25mV[13]. At higher surface potentials, this equation appears to be a good approximation for separation distances that are greater than 3 nm in 10 mM KCl, based on Table 1 of the referenced article[13]. Since the interaction energy barriers of highly charged particles in Figures S1 and S2 extend past 3 nm, the EDL equation is considered valid. Another requirement for the validity of the EDL equation is that the double layer thickness be small relative to the particle size, which is easily satisfied for the limiting condition of CuO nanoparticles in 10 mM KCl.

References Cited

1. Redman, J.A., S.L. Walker, and M. Elimelech, *Bacterial Adhesion and Transport in Porous Media: Role of the Secondary Energy Minimum.* Environmental Science & Technology, 2004. **38**(6): p. 1777-1785.
2. Baran, W., A. Makowski, and W. Wardas, *The effect of UV radiation absorption of cationic and anionic dye solutions on their photocatalytic degradation in the presence TiO2.* Dyes and Pigments, 2008. **76**(1): p. 226-230.
3. Begot, C., et al., *Recommendations for calculating growth parameters by optical density measurements.* Journal of Microbiological Methods, 1996. **25**(3): p. 225-232.
4. Mayton, H.M., I.M. Marcus, and S.L. Walker, *Escherichia coli O157: H7 and Salmonella Typhimurium adhesion to spinach leaf surfaces: Sensitivity to water chemistry and nutrient availability.* Food Microbiology, 2019. **78**: p. 134-142.
5. Waller, T., I.M. Marcus, and S.L. Walker, *Influence of septic system wastewater treatment on titanium dioxide nanoparticle subsurface transport mechanisms.* Analytical and bioanalytical chemistry, 2018: p. 1-8.
6. Elimelech, M. and C.R. O'Melia, *Effect of particle size on collision efficiency in the deposition of Brownian particles with electrostatic energy barriers.* langmuir, 1990. **6**(6): p. 1153-1163.
7. Vold, M.J., *Van der Waals' attraction between anisometric particles.* Journal of Colloid Science, 1954. **9**(5): p. 451-459.
8. Tufenkji, N. and M. Elimelech, *Deviation from the classical colloid filtration theory in the presence of repulsive DLVO interactions.* Langmuir, 2004. **20**(25): p. 10818-10828.
9. Bradford, S.A., J. Simunek, and S.L. Walker, *Transport and straining of E. coli O157: H7 in saturated porous media.* Water Resources Research, 2006. **42**(12).
10. Lanphere, J.D., et al., *Stability and transport of graphene oxide nanoparticles in groundwater and surface water.* Environmental engineering science, 2014. **31**(7): p. 350-359.
11. Elimelech, M., et al., *Relative insignificance of mineral grain zeta potential to colloid transport in geochemically heterogeneous porous media.* Environmental science & technology, 2000. **34**(11): p. 2143-2148.
12. Gregory, J., *Approximate expressions for retarded van der Waals interaction.* Journal of Colloid and Interface Science, 1981. **83**(1): p. 138-145.
13. Hogg, R., T.W. Healy, and D. Fuerstenau, *Mutual coagulation of colloidal dispersions.* Transactions of the Faraday Society, 1966. **62**: p. 1638-1651.